CsI(Tl) for WIMP dark matter searches

V. A. Kudryavtsev, N. J. C. Spooner, D. R. Tovey, J. W. Roberts, M. J. Lehner, J. E. McMillan, P. K. Lightfoot, T. B. Lawson, C. D. Peak, R. Lüscher

Department of Physics and Astronomy, University of Sheffield, Sheffield S3 7RH, UK

J. C. Barton

Birkbeck College, London WC1E 7HX, UK

Abstract

We report a study of CsI(Tl) scintillator to assess its applicability in experiments to search for dark matter particles. Measurements of the mean scintillation pulse shapes due to nuclear and electron recoils have been performed. We find that, as with NaI(Tl), pulse shape analysis can be used to discriminate between electron and nuclear recoils down to 4 keV. However, the discrimination factor is typically (10-15)% better than in NaI(Tl) above 4 keV. The quenching factor for caesium and iodine recoils was measured and found to increase from 11% to $\sim$ 17% with decreasing recoil energy from 60 to 12 keV. Based on these results, the potential sensitivity of CsI(Tl) to dark matter particles in the form of neutralinos was calculated. We find an improvement over NaI(Tl) for the spin independent WIMP-nucleon interactions up to a factor of 5 assuming comparable electron background levels in the two scintillators.

PACS: 29.40.Mc, 14.80.Ly, 95.25.+d, 95.30.Cq
Keywords: Scintillation detectors; Inorganic crystals; CsI(Tl) crystals; Dark matter; WIMP; Pulse shape discrimination

Corresponding author: V. A. Kudryavtsev, Department of Physics and Astronomy, University of Sheffield, Hicks Building, Hounsfield Rd., Sheffield S3 7RH, UK
Tel: +44 (0)114 2224531; Fax: +44 (0)114 2728079;
E-mail: v.kudryavtsev@sheffield.ac.uk

1. Introduction

NaI(Tl) crystals are widely used in searches for Weakly Interacting Massive Particles (WIMPs) - possible constituents of the galactic dark matter (see for example [1, 2, 3, 4]). However, a particular disadvantage of such crystals is their hygroscopic nature. This results in handling problems, in particular degradation of the surfaces through contact with moisture (such as from air humidity), which in turn increases the potential for generating atypical events from background electron or alpha interactions at the crystal surfaces [3, 5, 6]. CsI(Tl) crystals are much less hygroscopic than NaI(Tl) and hence offer a potential alternative with these surface complications reduced.

In this paper we report studies of the properties of CsI(Tl) relevant to its use as a possible detector for dark matter. To compete, or improve on, the sensitivity of NaI(Tl) to WIMP interactions CsI(Tl) needs to satisfy several requirements: i) it should provide discrimination between electron and nuclear recoils down to low energies (2-4 keV) using pulse shape analysis, ii) the quenching factor of caesium and iodine recoils should not be less than 10%, and iii) the background rate should be comparable to that achieved in low background NaI(Tl) crystals (1-2 dru, differential rate unit, 1 dru = 1 event/kg/day/keV). Our study here has concentrated on requirements i) and ii) since requirement iii), the background rate, is not an intrinsic property of CsI(Tl) but rather will vary from crystal to crystal depending on the selected starting materials, purification and manufacturing processes used (see Section 5). Recently, similar studies have been performed by Kim et al. [7] and Pécourt et al. [8]. Pécourt et al. [8] used a high energy neutron beam to measure quenching factors of nuclear recoils in CsI(Tl). Results indicate an increase in scintillation efficiency with decreasing recoil energy down to 25 keV suggesting CsI(Tl) detectors may be more favourable for dark matter searches than had previously been realised. They also measured distributions of mean scintillation pulse decay times induced by electron and nuclear recoils down to 5 keV and found better discrimination compared to NaI(Tl) crystals. In this work we have extended measurements of quenching factor down to recoil energies of 12 keV and have made detailed studies of the pulse shape and of the distribution of decay time constants due to electron and neutron induced recoils down to 2 keV. Finally, based on results of these studies we have estimated the discrimination efficiency achievable with CsI(Tl) and hence the sensitivity of CsI(Tl) to the spin independent WIMP-nucleon and spin dependent WIMP-proton interactions assuming various intrinsic background rates.

2. Mean pulse shapes

Measurements of the scintillation pulse characteristics of CsI(Tl) were achieved using a crystal of 3 inch diameter $\times$ 1.5 inch close coupled to two 3 inch ETL 9265KB photomultiplier tubes (PMTs). The crystal was polished and its curved surface wrapped in PTFE to provide a reflective coating. A light yield of about 5.5 photoelectrons (p.e.) / keV was achieved with this detector. Note that the choice of PMT was made here with respect to low background characteristics - the 9265KB (bialkali photocathode) being our standard choice in NaI(Tl) dark matter experiments. PMTs with optimum spectral response matched to the CsI(Tl) peak emission at 550 nm [9] would have higher quantum efficiency at this wavelength ($\sim$ 25% compared with $\sim$ 10% for bialkali) but are not available with known low background characteristics. Three different radioactive sources were used in the pulse shape experiments: a ^{57}Co gamma source (122 keV) for energy calibration; a

^{60}Co source to provide populations of low energy Compton scatter electrons; and a ^{252}Cf neutron source to produce nuclear recoil events. The energy resolution was found to be 7% at 122 keV, which exceeds the 'statistical resolution' calculated for a light yield of 5.5 p.e./keV, by a factor of 2 only. The measurements were performed mainly at a controlled temperature of $(10.0 \pm 0.5)^\circ$ C, to reduce PMT noise, and at room temperature $(23 \pm 1)^\circ$ C for comparison.

Mean pulse shapes for electron- and nuclear recoil- induced events for measured energies of 5-6 keV are shown in Figure 1. The pulse shape for nuclear recoil events is scaled down by a factor of 10 to avoid overlap of the two distributions. The energy range of 5-6 keV is chosen here because only at low energies do the nuclear recoils induced by neutrons from ^{252}Cf dominate over electron recoils induced by the accompanying gammas (the fraction of electron pulses does not exceed 2% at 5-6 keV). Two prominent decay components (fast and slow) are clearly seen in both distributions shown in Figure 1. This agrees with early measurements performed at high energies (see [10, 11, 12, 13] and references therein). The mean pulse shapes were found to be well fitted by the sum of two exponential components with time constants at 10° C of $\tau_{g1} = (860 \pm 60)$ ns, $\tau_{g2} = (2600 \pm 140)$ ns for gamma-induced pulses and $\tau_{n1} = (750 \pm 20)$ ns, $\tau_{n2} = (1800 \pm 100)$ ns for neutron-induced pulses.

3. Pulse shape discrimination

In further tests we have applied the standard procedure of pulse shape analysis adopted by the UK Dark Matter Collaboration for NaI(Tl) dark matter detectors [1, 5, 6, 14]. Pulses from both PMTs were integrated using a buffer circuit and then digitised using a LeCroy 9350A oscilloscope driven by a Macintosh computer running Labview-based data acquisition software. The digitised pulse shapes were passed to the computer and stored on disk. Final analysis was performed on the sum of the pulses from the two PMTs.

Our standard procedure of data analysis, described in [1], involves the fitting of a single exponential to each integrated pulse to obtain the index of the exponent, τ. Although scintillation pulses from CsI(Tl) have an additional second component (see Section 2), the pulses can nevertheless be well fitted by a single exponential if fits are restricted to data below 1500 ns (see Figure 1). This fraction of the pulse contains the major contribution to the integrated pulse amplitude so that the distortion of the fit due to the presence of the second exponential at large time scales was found to be insignificant. This approximation has the advantage that a three parameter fit can be used on each pulse and a simple discrimination parameter defined, rather than a considerably more complicated six parameter fit in the case of two decay constants. The free fit parameters used are: the time constant of the single exponent, τ; a normalisation constant and the start time of the pulse.

For each experiment (with gamma or neutron source) the distribution of the number of events versus the time constant of the exponent (τ) was generated for a range of energy bins. τ-Distributions for each population of pulses can be approximated by a gaussian in $\ln(\tau)$ [1, 5] (for a more detailed discussion of the distributions see [14] and references therein):

$$\frac{dN}{d\tau} = \frac{N_o}{\tau\sqrt{2\pi}\ln w} \cdot \exp\Big[\frac{-(\ln\tau - \ln\tau_o)^2}{2(\ln w)^2}\Big] \qquad (1)$$

The τ-distributions have been fitted with a gaussian in $\ln(\tau)$ with several free parameters as follows. For distributions from the ^{60}Co gamma source a 3-parameter fit was used with free parameters τ_o, w and N_o. In the experiments with the ^{252}Cf neutron source both neutrons and gammas (from the source as well as from local radioactivity) are detected. The resulting τ-distribution is thus fitted with two gaussians. However, the parameters τ_o and w for events initiated by Compton electrons are known from experiments with the ^{60}Co gamma source. Assuming the value of w (called the width parameter) for the nuclear recoil distribution is the same as that of the gamma distribution (since the width is determined mainly by the number of photoelectrons) again a 3-parameter fit can be applied [5]. In this case the free parameters are the number of neutrons, N_{on}, number of gammas, N_{og}, and the mean value of the exponent for the neutron distribution, τ_{on}.

Examples of τ-distributions of electron and nuclear recoils together with the gaussian fits are shown in Figure 2 for measured energies 8-9 keV. Note again, that both nuclear and electron recoil pulses are present in the τ-distribution obtained with the neutron source (see also [5]) (the contribution of electron recoils is shown by dashed line).

The mean values τ_o of log-gaussian fits as a function of measured energy are shown in Figure 3 for electron and nuclear recoils and for two temperatures of the crystal, 23° C (room temperature) and 10° C. There is a strong energy and temperature dependence of the parameter τ_o. However, the fact that the values of τ_o increase with decreasing temperature is found not to influence the discrimination (see below) since the ratio of nuclear to electron recoil time constants and the width parameter remain almost constant.

The ratio of nuclear to electron recoil time constants as a function of energy for 10° C is shown in Figure 4 in comparison with values for NaI(Tl) [15]. The lower ratio of time constants found in the CsI(Tl) crystal results in better discrimination between nuclear and electron recoils than in NaI(Tl). The real gain is reduced due to the larger value of the width w for CsI(Tl), shown in Figure 5. No discrimination was found below 4 keV, which is true also for NaI(Tl) crystals.

The ratio of time constants at 10° C is found empirically to be approximated by: R_τ ($E > 4$ keV)$= a + b \cdot \exp[(c - E)/d]$ and R_τ ($E < 4$ keV) $= 1$, where the parameters are: $a = 0.65$, $b = 0.35$, $c = 3$ keV and $d = 4.5$ keV for the CsI(Tl) crystal and $a = 0.75$, $b = 0.25$, $c = 3$ keV and $d = 5$ keV for NaI(Tl) [15]. The parameterisations are shown in Figure 3 by solid lines. The width w of the τ-distribution is a function of the number of photoelectrons and can be parameterised as: $w = 1 + f \cdot (N_{pe})^{-1/2}$, where N_{pe} is the number of photoelectrons and parameter $f = 2.4$ for CsI(Tl) at 10° C and $f = 1.7$ for NaI(Tl) at 10° C [15]. Note that the dependence of parameter f on the crystal and its temperature was found to be insignificant for NaI(Tl) crystals.

To quantify the discrimination between nuclear and electron recoils we define a discrimination factor $D = 1 - S$, where S is the fraction of the electron and nuclear recoil τ-distributions that are overlapping - the distributions being first normalised to a total count of 1 [15]. For fully overlapping distributions, $R_\tau = 1$ and $D = 0$ and there is no discrimination. For separated distributions $D = 1$ and there is full event by event discrimination. The discrimination factors as a function of measured energy are shown in Figure 6 for CsI(Tl) and NaI(Tl) detectors with different light yields derived using the aforementioned parameterisations of R_τ and w. It can be seen from Figure 6 that for a given light yield, above ~ 4 keV, the discrimination power of CsI(Tl) is always better than that of NaI(Tl), typically by $\sim (10 - 15)\%$.

4. Quenching factor

The measurement of scintillation efficiency or quenching factor of caesium and iodine recoils in CsI(Tl) was performed using the 2.85 MeV neutron beam facility of Sheffield University with 1 inch diameter × 1 inch CsI(Tl) crystal. The experimental set up and analysis procedure adopted was similar to that described in [14, 16]. Neutrons were scattered through angles of (45–120) degrees with respect to the primary flux, yielding nuclear recoil energies of 12.5–65 keV. As the masses of caesium and iodine nuclei are very similar, discrimination between them was not possible so the results obtained refer to both types of nuclei.

The measured quenching factor $Q = E_m/E_r$, where E_m is measured energy and E_r is recoil energy, is shown in Figure 7a as a function of recoil energy together with the measurement reported in [8]. There is a good agreement between the two measurements. Both measurements indicate an increase in quenching factor with decreasing recoil energy. This important result significantly affects the WIMP sensitivity of CsI(Tl) crystals (see Section 5), in particular to spin independent interactions for which the recoil spectrum falls most rapidly with energy. To calculate the sensitivities to WIMP interactions the dependence of the quenching factor on the recoil energy was converted to measured energy versus recoil energy. This is shown in Figure 7b together with our empirical parameterisation.

5. Sensitivity of CsI(Tl) detectors to WIMP search

Taking the results of the measurements reported above, we can calculate the potential sensitivity of CsI(Tl) to WIMP-proton spin dependent and WIMP-nucleon spin independent interactions. Another parameter, which is important in such calculations, is the background rate. As mentioned in Section 1, this is an uncertain parameter, since the background rate (for instance, if determined by ^{137}Cs, ^{135}Cs and ^{134}Cs contamination) is a property of the particular crystal used and may vary by an unknown factor from one crystal to another. Therefore, in our simulations we have chosen, for illustrative purposes, to use two values of background rate: 2 dru and 10 dru. The first one is the background rate reached currently in low-background NaI(Tl) detectors used to search for dark matter particles in the form of neutralinos [2, 3, 15]. The second one is a more realistic estimate of the background in the CsI(Tl) contaminated with radioactive isotopes of ^{137}Cs, ^{135}Cs and ^{134}Cs. We have assumed in the simulations that the energy threshold was 2 keV, the light yield is 3 p.e./keV, the discrimination between nuclear and electron recoils starts at 4 keV and the parameters of the log-gaussian fits are as described above. We have used our empirical parameterisation for the relation between measured energy and recoil energy, shown in Figure 7b. The spin factor of ^{133}Cs has been calculated using the odd group model [17]. The spin-dependent form factor and spin factor for iodine have been taken from [17, 18, 19] and the spin dependent form factor for caesium has been assumed to be the same as for iodine. A higgsino-type neutralino has been assumed. The form factors for caesium and iodine for spin independent interactions have been calculated using Helm's parameterisation [20] (see also the discussion in [19]). An A^2-enhancement of the spin independent cross-section has been assumed. The halo parameters have been taken as follows: local dark matter density $\rho_{dm} = 0.3$ GeV/cm^3, the Maxwellian dark matter velocity distribution with $v_o = 220$ km/s, the local Galactic escape velocity $v_{esc} = 650$ km/s and the Earth's velocity relative to the dark matter distribution $v_{Earth} = 232$ km/s.

The resulting sensitivity plots are presented in Figures 8a and 8b for spin dependent

and spin independent interactions, respectively. It can be seen that no improvement in sensitivity is expected from CsI(Tl) compared with NaI(Tl) for spin-dependent WIMP-proton interactions even when the lower background rate is assumed. This is due to the step nature of the form factor functions of both caesium and iodine, while that of sodium is smoother resulting in a dominant contribution from sodium interactions in NaI(Tl) detectors. (Note that more precise calculations of the caesium spin factor may modify the sensitivity curve but are unlikely to change the conclusion). However, it is found that CsI(Tl) (even with higher background rate) is more sensitive to spin independent interactions than NaI(Tl) at a given light yield. This is because both caesium and iodine nuclei have large mass and hence the WIMP-nucleus interaction rate is affected by a large A^2-enhancement factor. The increase in nuclear recoil scintillation efficiency with decreasing energy also contributes to the improvement in the sensitivity.

6. Conclusions

Measurements of various characteristics of CsI(Tl) relevant to dark matter searches have been performed in the range of visible energies 2-20 keV - important for WIMP-nucleus interactions. Discrimination between nuclear and electron recoils was found to be typically (10-15)% better than in NaI(Tl) crystals for a given light yield and the scintillation efficiency factor for caesium and iodine recoils was found to increase with decreasing recoil energy, in good agreement with the results reported in [8]. Based on these results the sensitivity of CsI(Tl) to spin independent WIMP-nucleon interactions appears to be better than that of NaI(Tl) up to a factor of 5 for a given light yield assuming that the background rate achievable in CsI(Tl) can be similar to that found in low background NaI(Tl) crystals. For spin dependent WIMP-proton interactions the sensitivity of CsI(Tl) appears to be worse than that of NaI(Tl).

Based on these conclusions it appears that CsI(Tl) could provide a dark matter target with similar or improved sensitivity over NaI(Tl) but with the additional advantage of easier control over potential surface background events. However, there remains the need to assess the intrinsic electron background in CsI(Tl) in particular that due to ^{137}Cs. This, and investigation of the application of radiopurification techniques used in NaI to CsI, will be the subject of future studies.

7. Acknowledgements

The authors wish to thank the following for their support: PPARC, Electron Tubes Ltd. (J.E.M.), Royal Society (R.L., ESEP grant N 81RS-57440). We are grateful to D. Lewin (RAL) for useful discussions.

References

[1] P. F. Smith et al. *Phys. Lett. B*, **379** (1996) 299

[2] R. Bernabei et al. *Phys. Lett. B*, **389** (1996) 757

[3] G. Gerbier et al. *Astroparticle Phys.*, **11** (1999) 287

[4] K. Fushimi et al. *Astroparticle Phys.*, **12** (1999) 185

[5] V. A. Kudryavtsev et al. *Phys. Lett. B*, **452** (1999) 167

[6] N. J. T. Smith et al. *Phys. Lett. B*, **467** (1999) 132

[7] H. J. Kim et al. physics/9910044, submitted to *Nucl. Instrum. and Meth. in Phys. Res. A*

[8] S. Pécourt et al. *Astroparticle Phys.*, **11** (1999) 457

[9] H. Grassmann et al. *Nucl. Instrum. and Meth. in Phys. Res.*, **228** (1985) 323

[10] J. B. Birks. The theory and practice of scintillation counting (Pergamon Press, 1964)

[11] J. D. Valentine et al. *IEEE Trans. Nucl. Sci.*, **40** (1993) 1267

[12] P. Schotanus et al. *IEEE Trans. Nucl. Sci.*, **37** (1990) 177

[13] F. Benrachi et al. *Nucl. Instrum. and Meth. in Phys. Res.*, **281** (1989) 137

[14] D. R. Tovey. Ph. D. Thesis, University of Sheffield (1998)

[15] N. J. C. Spooner et al. *Phys. Lett. B*, **473** (2000) 330.

[16] D. R. Tovey et al. *Phys. Lett. B*, **433** (1998) 150

[17] J. D. Lewin. Rutherford Appleton Laboratory. Private communication.

[18] M. T. Ressel and D. J. Dean. *Phys. Rev. C*, **56** (1997) 535

[19] J. D. Lewin and P. F. Smith. *Astroparticle Phys.*, **6** (1996) 87

[20] R. H. Helm. *Phys. Rev.*, **104** (1956) 1466

Figure captions

Figure 1. Mean pulse shapes of nuclear and electron recoil pulses in CsI(Tl) crystal for measured energy 5-6 keV. Pulse shape of nuclear recoils is scaled down by a factor of 10. Fits with two exponential components to the measured distributions are shown by solid curves.

Figure 2. Time constant distributions of nuclear and electron recoil pulses: a) τ-distribution measured with gamma source; b) τ-distribution measured with neutron source. Nuclear and electron recoil pulses are present in b). Fits with one (a) or two (b) log-gaussian components are shown by solid curves. Contribution of gamma-induced pulses is shown by dashed curve in b).

Figure 3. Mean time constants of log-gaussian distributions versus measured energy are shown for nuclear and electron recoils at different temperatures: crosses – nuclear recoils at room temperature; squares – electron recoils at room temperature; triangles – nuclear recoils at 10° C; diamonds – electron recoils at 10° C.

Figure 4. Ratio of nuclear to electron mean time constant for CsI(Tl) (diamonds) and NaI(Tl) (triangles) crystals at 10° C together with empirical parameterisations.

Figure 5. Width of log-gaussian distributions as a function of measured energy for CsI(Tl) (diamonds) and NaI(Tl) (triangles) crystals at 10° C together with empirical parameterisations.

Figure 6. Discrimination factor as a function of measured energy for CsI(Tl) (squares – light yield = 3 p.e./keV, triangles – light yield = 8 p.e./keV) and NaI(Tl) (diamonds – light yield = 3 p.e./keV, crosses – light yield = 8 p.e./keV) from [15] (see text for details).

Figure 7. a) Quenching factor of nuclear recoils in CsI(Tl) crystal as a function of recoil energy (squares) is shown together with the results from [8] (triangles). b) Visible energy versus recoil energy: squares – present data, triangles – data from [8], solid line - empirical parameterisation.

Figure 8. Estimates of the sensitivity of CsI(Tl) detector with 10 kg×years exposure to a) spin dependent WIMP-proton and b) spin independent WIMP-nucleon interactions compared with NaI(Tl) detector [15]: a) solid curve - our estimates for CsI(Tl) crystal with a background rate of 2 dru and light yield 3 p.e./keV, dashed curve - UKDMC limits from [1] recalculated [15] with new halo parameters and spin factors, dotted curve - estimates for NaI(Tl) crystal [15] for light yield 3 p.e./keV; b) solid curve - our estimates for CsI(Tl) crystal with a background rate of 2 dru and light yield 3 p.e./keV, dash-dotted curve – our estimates for CsI(Tl) crystal with a background rate of 10 dru and light yield 3 p.e./keV, dashed curve - UKDMC limits from [1] recalculated [15] with new halo parameters and spin factors, dotted curve - estimates for NaI(Tl) crystal [15] for light yield 3 p.e./keV; (see also text for details).

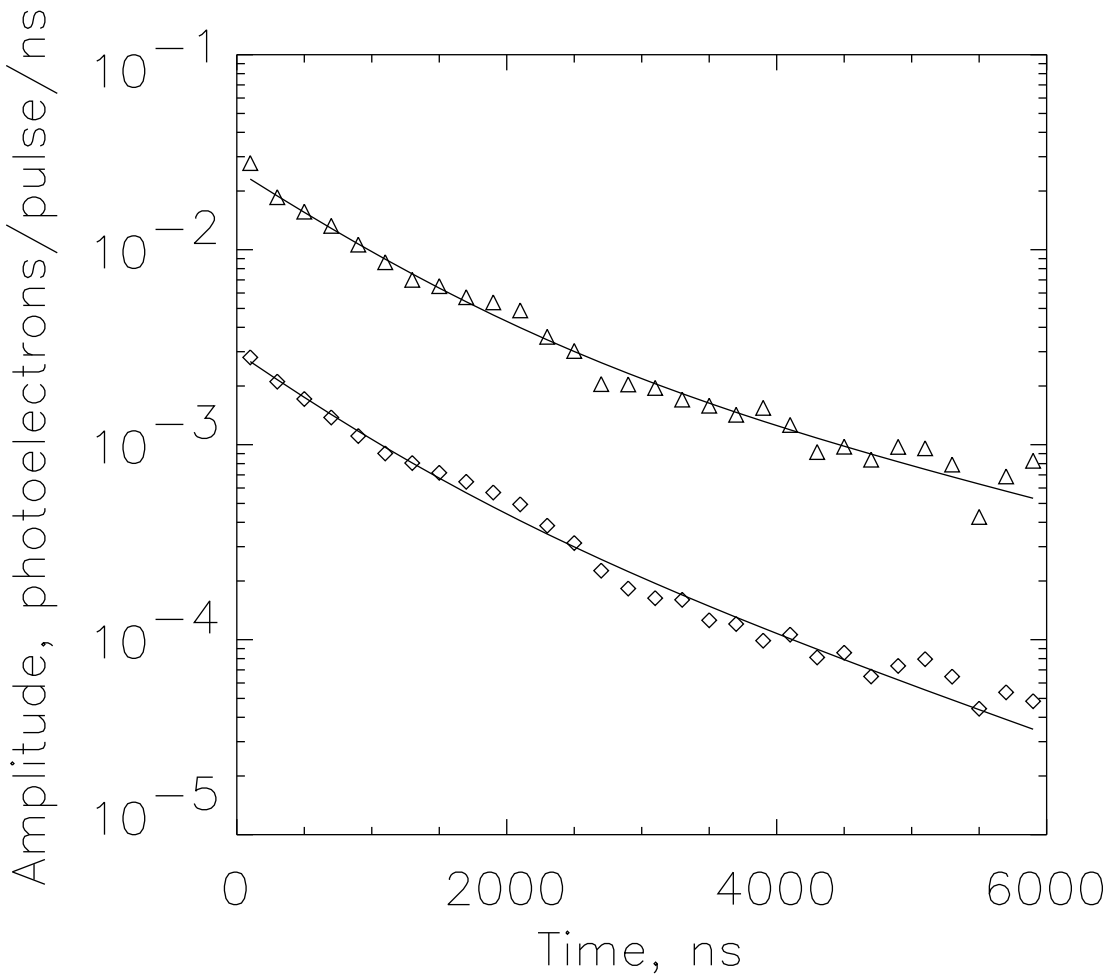
Amplitude, photoelectrons/pulse/ns
10^{-1}
10^{-2}
10^{-3}
10^{-4}
10^{-5}
0
2000
4000
6000
Time, ns

Figure 1:

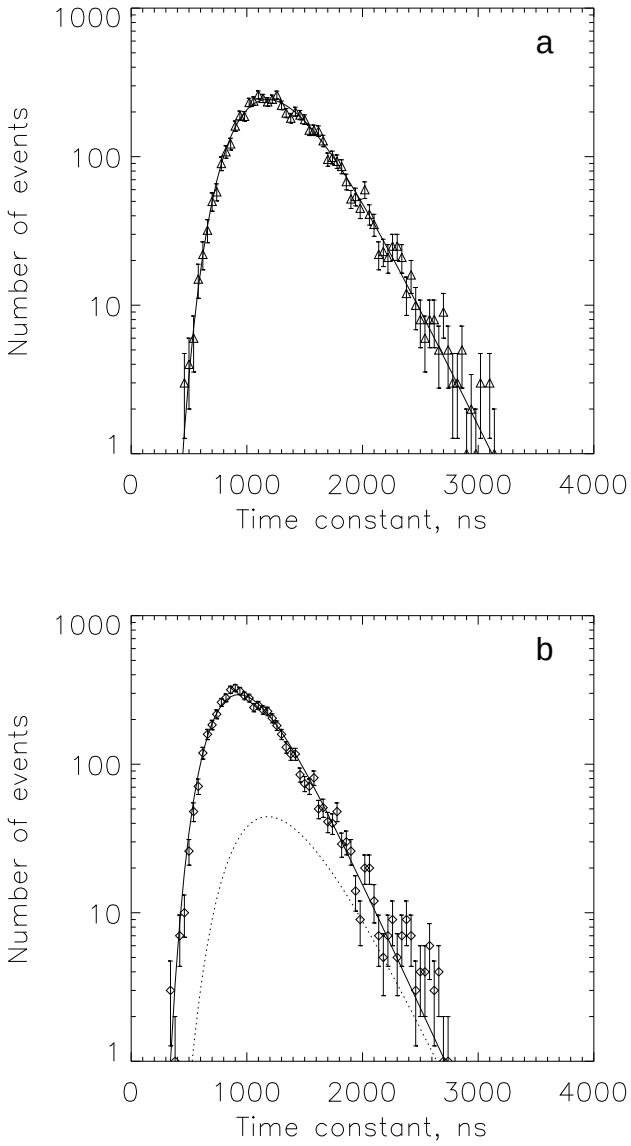
a
b
Number of events
Time constant, ns
1000
100
10
1
0
1000
2000
3000
4000

Figure 2:

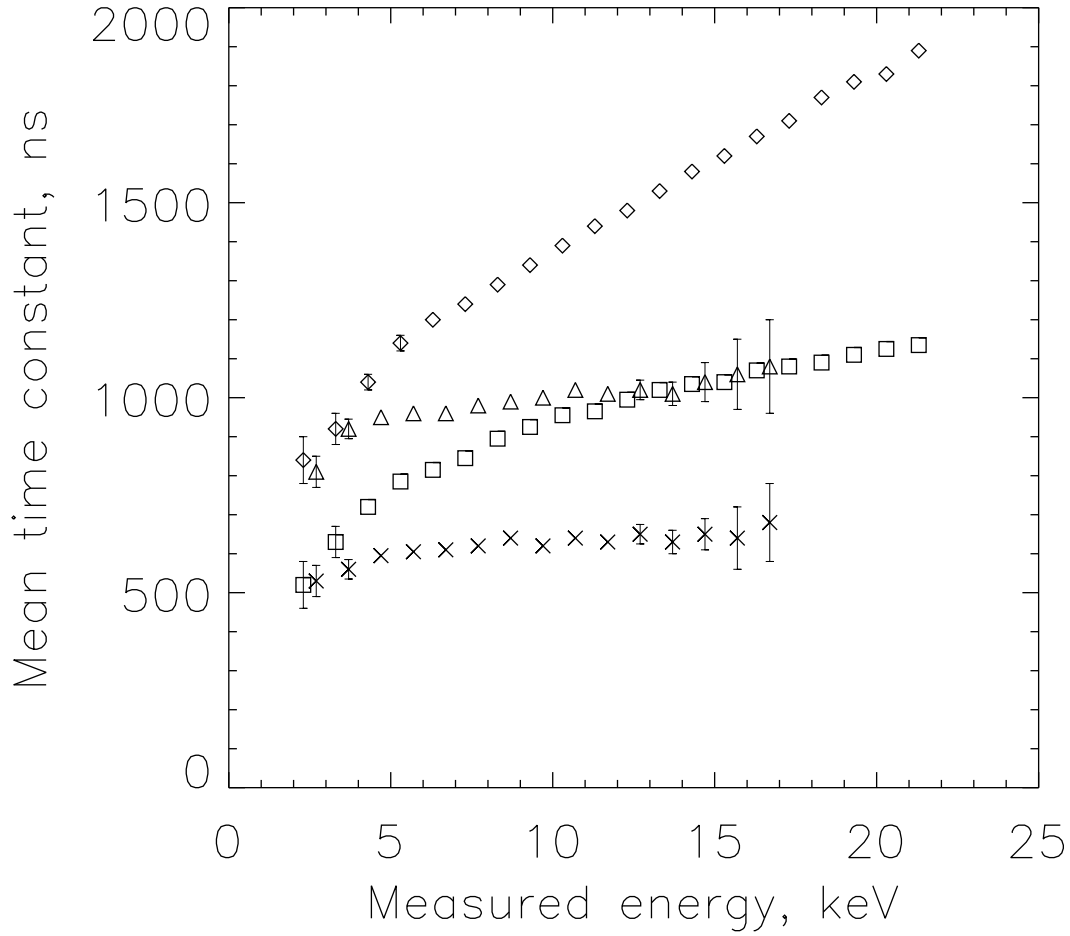
2000
1500
1000
500
0
Mean time constant, ns
0
5
10
15
20
25
Measured energy, keV

Figure 3:

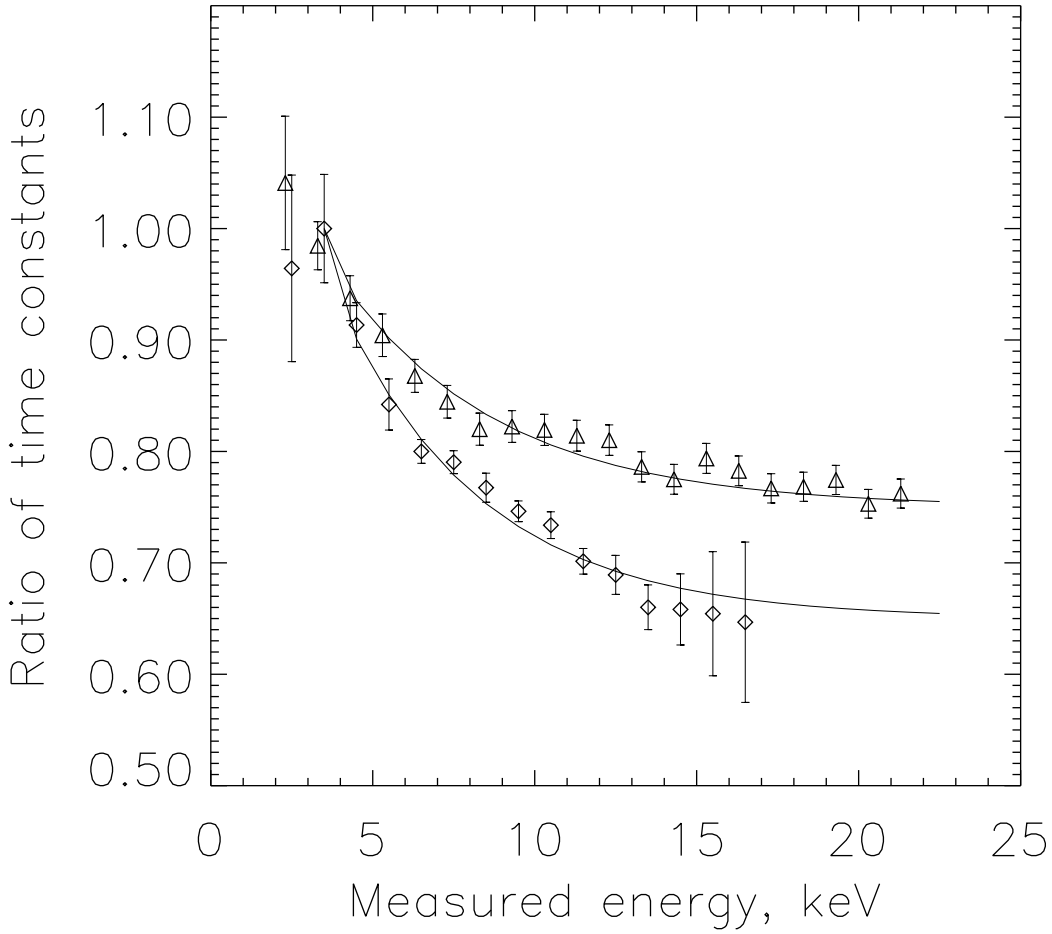
Ratio of time constants
1.10
1.00
0.90
0.80
0.70
0.60
0.50
0
5
10
15
20
25
Measured energy, keV

Figure 4:

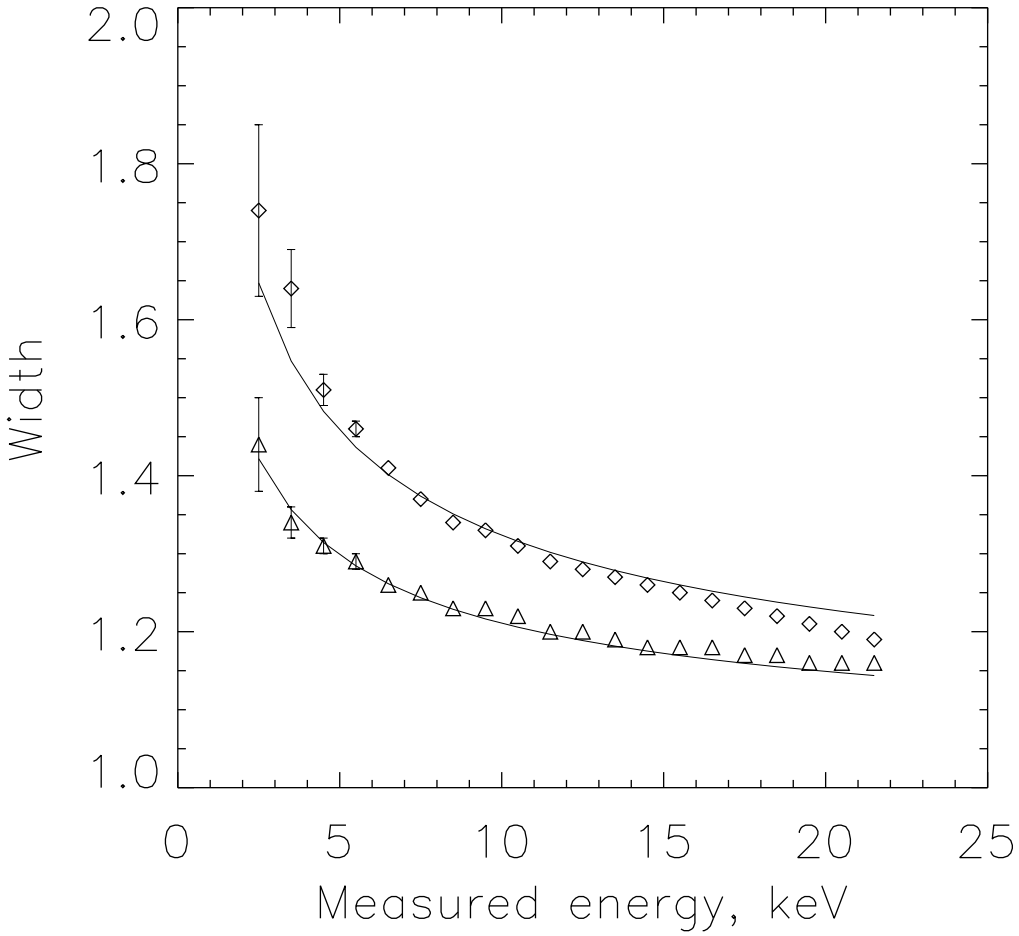

Figure 5:

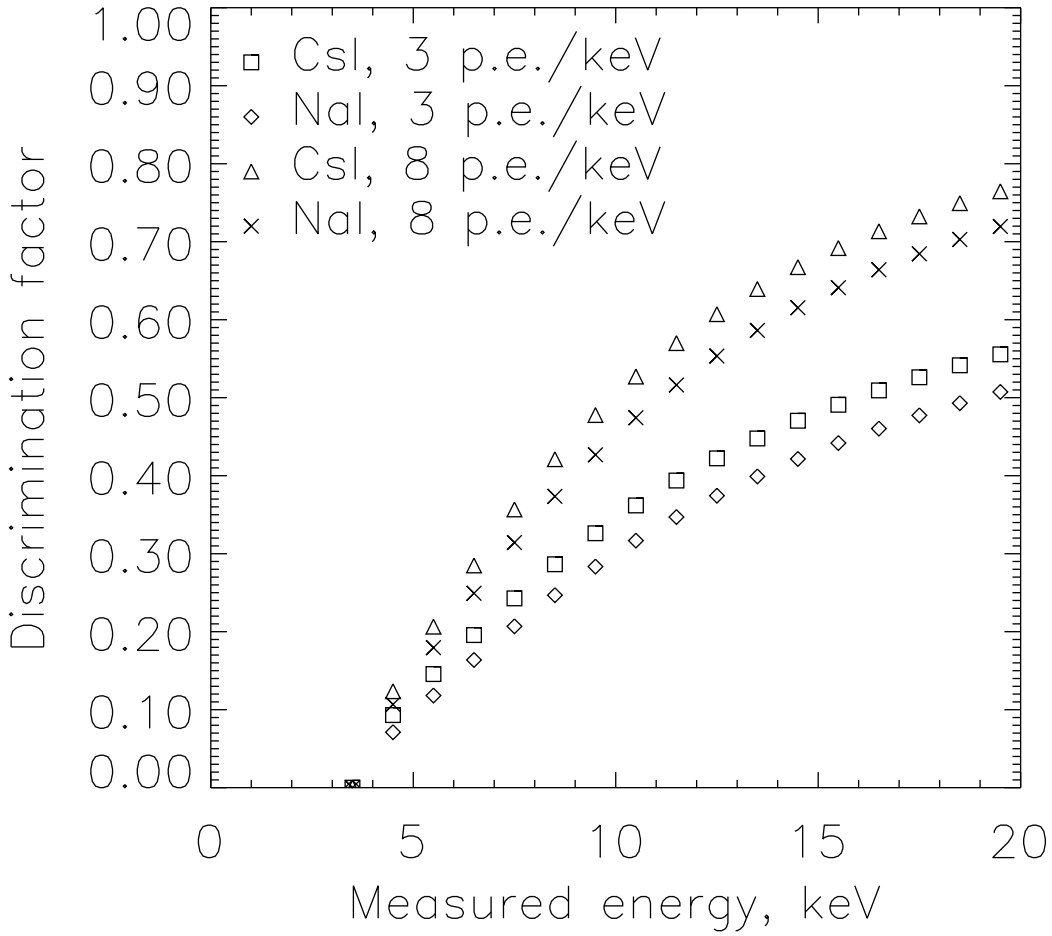
1.00
0.90
0.80
0.70
0.60
0.50
0.40
0.30
0.20
0.10
0.00
Discrimination factor
CsI, 3 p.e./keV
NaI, 3 p.e./keV
CsI, 8 p.e./keV
NaI, 8 p.e./keV
0
5
10
15
20
Measured energy, keV

Figure 6:

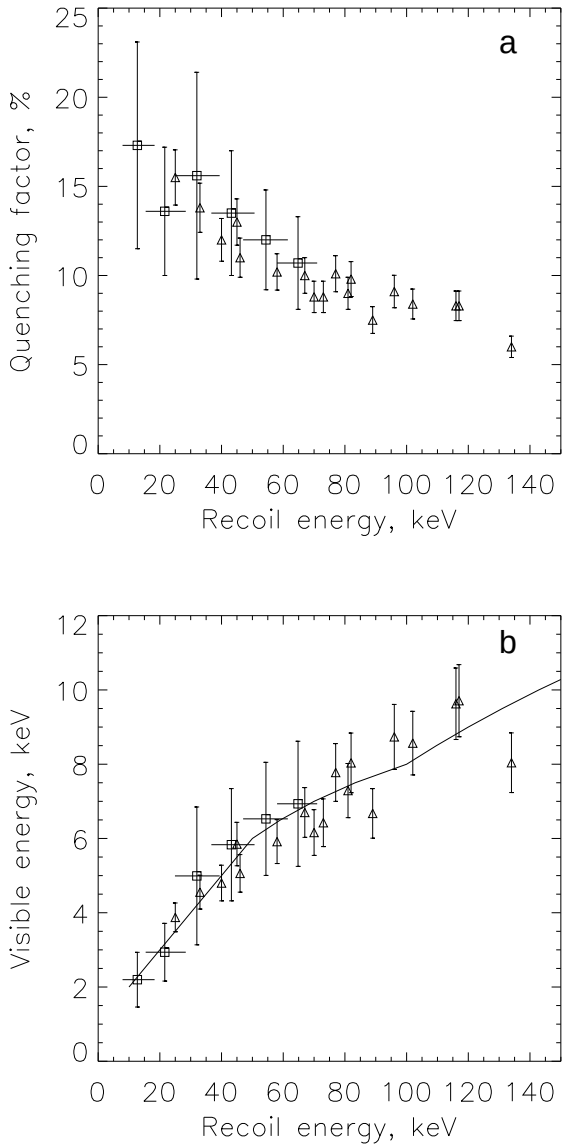
a
Quenching factor, %
Recoil energy, keV
b
Visible energy, keV
Recoil energy, keV

Figure 7:

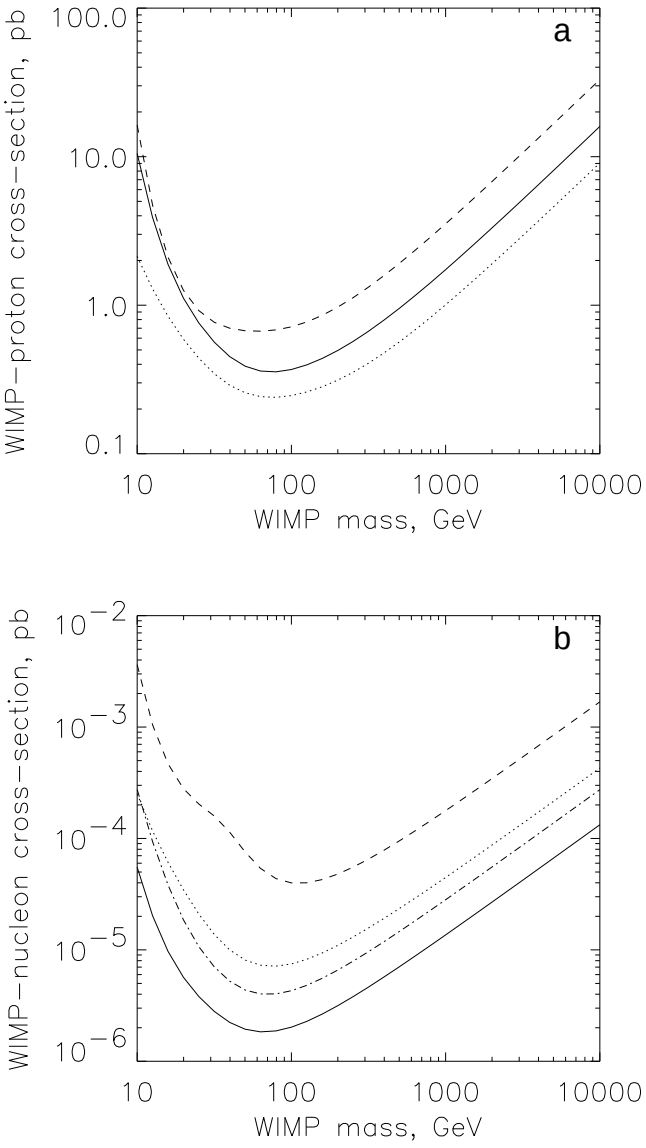
a
WIMP−proton cross−section, pb
100.0
10.0
1.0
0.1
10
100
1000
10000
WIMP mass, GeV
b
WIMP−nucleon cross−section, pb
10^{-2}
10^{-3}
10^{-4}
10^{-5}
10^{-6}
10
100
1000
10000
WIMP mass, GeV

Figure 8: